

# Offshore killer whale tracking using multiple hydrophone arrays

Martin Gassmann,<sup>a)</sup> E. Elizabeth Henderson, and Sean M. Wiggins  
*Scripps Institution of Oceanography, 9500 Gilman Drive, La Jolla, California 92093-0205*

Marie A. Roch  
*Department of Computer Science, San Diego State University, 5500 Campanile Drive, San Diego, California 92182-7720*

John A. Hildebrand  
*Scripps Institution of Oceanography, 9500 Gilman Drive, La Jolla, California 92093-0205*

(Received 14 July 2012; revised 30 August 2013; accepted 19 September 2013)

To study delphinid near surface movements and behavior, two L-shaped hydrophone arrays and one vertical hydrophone line array were deployed at shallow depths (<125 m) from the floating instrument platform R/P FLIP, moored northwest of San Clemente Island in the Southern California Bight. A three-dimensional propagation-model based passive acoustic tracking method was developed and used to track a group of five offshore killer whales (*Orcinus orca*) using their emitted clicks. In addition, killer whale pulsed calls and high-frequency modulated (HFM) signals were localized using other standard techniques. Based on these tracks sound source levels for the killer whales were estimated. The peak to peak source levels for echolocation clicks vary between 170–205 dB re 1  $\mu$ Pa @ 1 m, for HFM calls between 185–193 dB re 1  $\mu$ Pa @ 1 m, and for pulsed calls between 146–158 dB re 1  $\mu$ Pa @ 1 m. © 2013 Acoustical Society of America. [<http://dx.doi.org/10.1121/1.4824162>]

PACS number(s): 43.30.Sf, 43.60.Jn, 43.60.Fg, 43.60.Uv [MS]

Pages: 3513–3521

## I. INTRODUCTION

Tracking odontocetes using acoustic arrays can provide insight into their abundance and submerged behavior. The use of towed hydrophone arrays for line transect surveys has become an accepted method for abundance estimation of sperm whales (Barlow and Taylor, 2005; Lewis *et al.*, 2007), or to study their submerged behavior (Thode, 2005). The towed array is used to determine the bearing to vocalizing animals; their range is often estimated by observing their change in bearing as the tow ship moves past the animals' location. An alternative for detailed localization is to use vector sensors to provide directional information from multiple array elements (Thode *et al.*, 2010), or to exploit multipath arrivals and interaction with range-dependent bathymetry (Tiemann *et al.*, 2006). Likewise, widely spaced (km-scale) seafloor arrays have been used to track sperm whales using their intense echolocation clicks (e.g., Nosal and Frazer, 2007). However, smaller cetaceans, such as delphinids, produce echolocation clicks at higher frequencies that attenuate quickly over distance. Since their clicks are highly directional, the same click is often not detected at multiple elements within a km-scale array. To track clicks from small cetaceans, a smaller aperture array is needed (e.g., Wiggins *et al.*, 2012).

In this paper, we describe a three-dimensional, propagation model-based tracking method which utilizes three small-aperture (meter-scaled) arrays deployed at shallow depths from the stationary Floating Instrument Platform

(FLIP) (Fisher and Spiess, 1963). The capabilities of this method are illustrated by tracking a group of five clicking offshore killer whales (*Orcinus orca*) over a horizontal range of several hundred meters at shallow depths (<40 m) in the refractive ocean environment of the Southern California Bight.

In addition to the impulsive, broad-band echolocation clicks used for foraging (Au *et al.*, 2004), killer whales produce pulsed calls and frequency-modulated whistles for communicative purposes (Ford, 1989) as well as high-frequency modulated (HFM) calls with frequencies well above the typical whistle frequency range (Samarra *et al.*, 2010; Simonis *et al.*, 2012). To provide a more complete representation of the killer whales' paths and acoustic behavior, their HFM and pulsed calls were localized using arrays of hydrophones separated by tens of meters and by a few kilometers, respectively.

## II. METHODS

### A. Experimental setup

The research platform FLIP was placed in a nearly stationary three-point mooring 7 km northwest of San Clemente Island in the Southern California Bight for 25 days during October and November 2008 (Fig. 1). FLIP provides a stable observation deck 25 m above the sea surface from which visual observers can monitor cetaceans as they surface to breathe, in addition to providing a persistent platform for deploying instrumentation such as hydrophone arrays for acoustic monitoring. Deployed from FLIP to record marine mammal sounds for tracking were three small aperture hydrophone arrays: two L-shaped arrays (L1 and L2) each

<sup>a)</sup>Author to whom correspondence should be addressed. Electronic mail: [mgassmann@ucsd.edu](mailto:mgassmann@ucsd.edu)

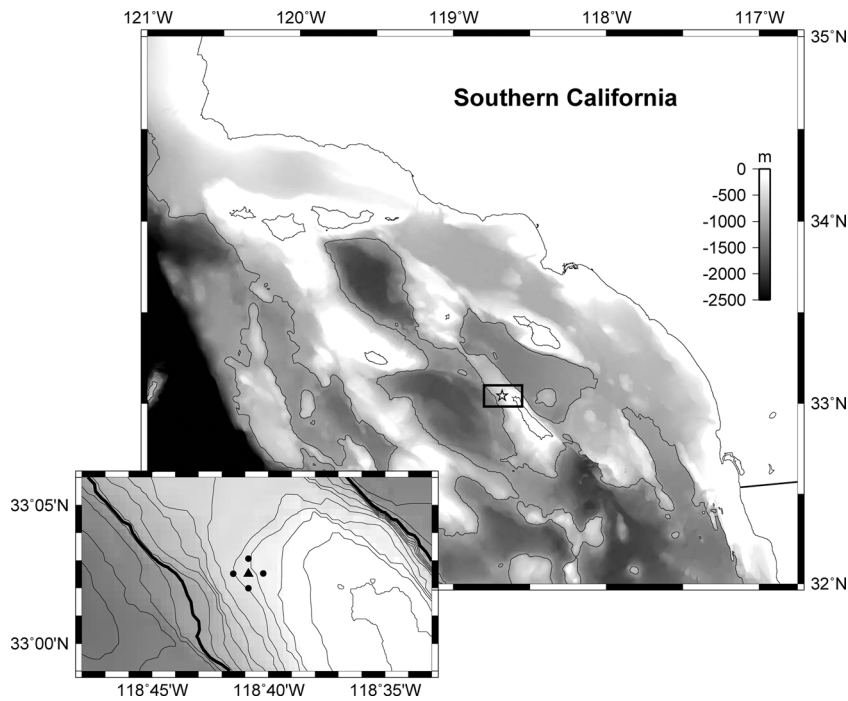


FIG. 1. Location of the FLIP (triangle) in the Southern California Bight north-west of San Clemente Island. Four HARPs (dots) are located 1 km north, east, south, and west of FLIP on the seafloor at 300–400 m depth. Bathymetry contours are every 200 m with the thick black contour at 1000 m.

with one vertical leg and one horizontal leg at 36 m depth, and one vertical line array (VLA) below the draft of FLIP at 122 m depth (Fig. 2). Combining either L1 or L2 with VLA provides a medium aperture array with 86 m sensor spacing allowing signals with longer durations than clicks to be localized. L1 and L2 were separated horizontally by 12 m and were 12 m from the hull of FLIP (three times the hull diameter) with a 5° bearing for the horizontal leg of L1 and 60° bearing for the horizontal leg of L2, relative to FLIP face. This configuration reduces the shadowing from the hull of FLIP while enabling unambiguous locations of sound sources near the sea surface. The small-aperture hydrophone

spacing of L1 and L2 are designed to be minimally redundant with spacings between 0.2 and 2.15 m, to process low and high-frequencies with a small number of hydrophones. The spacing of the VLA arrays elements is 1.2 m. All three arrays were constructed from omni-directional spherical hydrophones (HS-150 Sonar Research and Development, Ltd., Beverley, UK) with a flat sensitivity (+/- 2 dB) of -205 dB re V/μPa from 1 to 125 kHz. The 14 hydrophone signals were band-pass filtered from 2 to 96 kHz and amplified using 14 separate circuit boards, which were custom-designed and built. Each signal was sampled continuously at 192 kHz with 16 bit resolution using two 8-channel analog digital converters (ADCs) (MOTU 896, Cambridge, MA). The GPS (global positioning system) derived analog time code IRIG-B was sampled by one channel of both ADCs for time-synchronization. Each ADC was connected to a data acquisition computer streaming the eight digitized channels into WAVE files and stored onto hard disks continuously resulting in 15 TB of data recorded during the 25 days deployment.

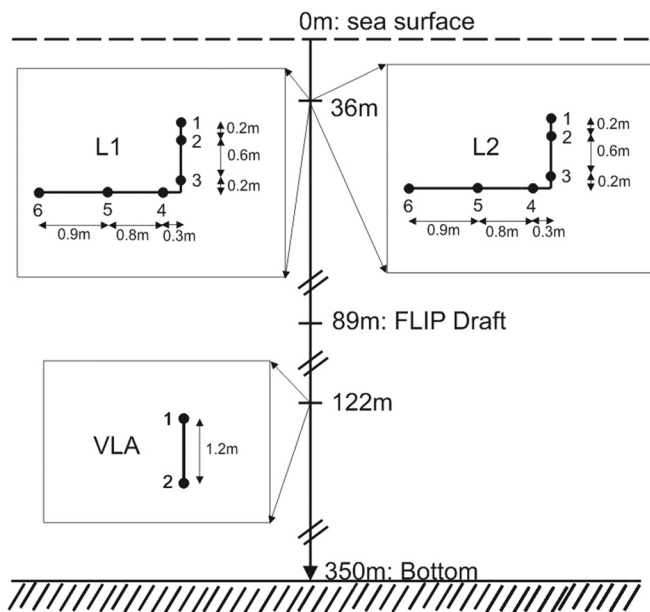


FIG. 2. Hydrophone array configuration. The two L-shaped arrays L1 and L2 are located 36 m below the sea surface on the port and starboard-side of FLIP, respectively. The VLA is located 86 m below the L-shaped arrays at 122 m depth.

To characterize the refractive ocean environment, daily sound velocity profiles based on temperature, pressure, and salinity (Chen and Millero, 1977) were obtained from deployments of a Seabird 29 CTD probe from FLIP.

A large aperture hydrophone array, consisting of four high-frequency acoustic recording packages (HARPs), was deployed near the seafloor (300–400 m depth) approximately 1 km north, east, south, and west of FLIP (Fig. 1). The four HARPs were each equipped with a single hydrophone, low-drift ( $10^{-8}$ ) synchronized clocks, and recorded continuously at a sampling frequency of 200 kHz (Wiggins and Hildebrand, 2007).

## B. Acoustic identification of killer whale sounds

The echolocation clicks and pulsed calls of killer whales have distinct characteristics, which together enable the

discrimination to species level (Barrett-Lennard *et al.*, 1996; Au *et al.*, 2004). The killer whales sounds recorded during this experiment were identified as the non-mammal eating offshore ecotype by an expert of killer whale sounds (personal communications, John Ford, University of British Columbia). However, no visual confirmation was possible since the killer whales passed by FLIP during night time. In addition, whistles could not be unambiguously distinguished from pulsed calls, so these types of sounds were all considered pulsed calls.

### C. Three-dimensional click localization

Impulsive, broad-band echolocation clicks were automatically detected in the recordings using a Teager energy detector on one channel of each array. Briefly, the Teager (Kaiser, 1990), or Teager–Kaiser energy, is a nearly instantaneous energy measurement whose discrete form can be computed from three samples. Teager energy responds rapidly to energy onset and was first proposed for marine mammal echolocation click detection by (Kandia and Stylianou, 2006). An independent implementation (Roch *et al.*, 2011) detects clicks based on thresholds derived from order statistics and uses a region growing procedure (e.g., similar to Fristrup and Watkins, 2004) to find the start and end of each echolocation click. Further details may be found in Roch *et al.* (2011). Vertical and horizontal angles were estimated from the vertical and horizontal hydrophones of the arrays using a time difference of arrival (TDOA) method as described below. Based on the TDOA obtained angles of the three arrays, range, depth, and bearing were computed and then transformed to a click location in a Cartesian coordinate system with FLIP as the center. The clicks were evaluated by an analyst and associated with a single track or excluded as outliers.

The localization algorithms and the orientation of L1 and L2 were verified by tracking the propulsion noise of a ship at known GPS positions approximately 350–500 m away with a horizontal bearing root-mean-square (rms) error of 3° and a range and depth rms error of 38 and 21 m, respectively.

#### 1. TDOA angle estimation

The broad-band echolocation clicks of delphinid species have an autocorrelation function with a highly pronounced peak and low side lobes due to their impulsive character in the time domain (Au *et al.*, 2004). Therefore, the TDOA ( $\Delta t$ ) of a click recorded on any two hydrophones can be computed by cross-correlating the time series. For a delphinid high-frequency click produced several hydrophone spacing away from the two hydrophones, a plane wave approximation can be used (Fig. 3). If the hydrophone spacing is  $d$  and the sound speed of the water is  $c$ , then the incident angle of the plane wave is

$$\beta = \cos^{-1} \left( \frac{c \cdot \Delta t}{d} \right). \quad (1)$$

#### 2. Range and depth

High-frequency clicks can be described as rays propagating in the refractive ocean environment characterized by a sound speed profile (Fig. 4). For each click, the TDOA-

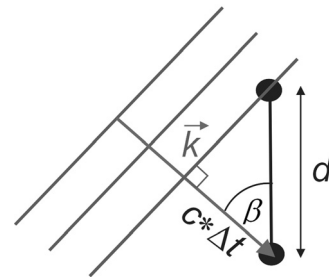


FIG. 3. The angle,  $\beta$ , of an incoming plane wave with wave number vector,  $\vec{k}$ , is the inverse cosine of the TDOA,  $\Delta t$ , and the speed of sound,  $c$ , divided by the distance between the two sensors,  $d$  [see Eq. (1)].

obtained vertical angles from the VLA at 122 m depth and from the vertical leg (hydrophones 1 and 3) of L2 at 36 m were used as start angles for two rays, which were then back-propagated in the range-depth space using the BELLHOP propagation model (Porter and Bucker, 1987). The intersection of the rays yields a unique depth and range estimate for each click by finding the range-depth pair of each ray with the smallest difference to each other, using the non-linear minimization algorithm Nelder–Mead simplex (Lagarias *et al.*, 1998).

Due to the high sensitivity of the vertical angles, especially at large ranges for L1 and L2 (1.7° difference for a range change from 400 to 300 m), the range and depth time series for tracked animals were smoothed using polynomials of the order 5–10.

Only the hydrophone pair 2–3 for L1 and 1–3 for L2 were used to obtain vertical angles due to temporarily and permanently malfunctioning hydrophones and significant differences in the noise levels between the hydrophones. Each of those hydrophone combinations represent the best possible mix of low noise floors and large apertures (high

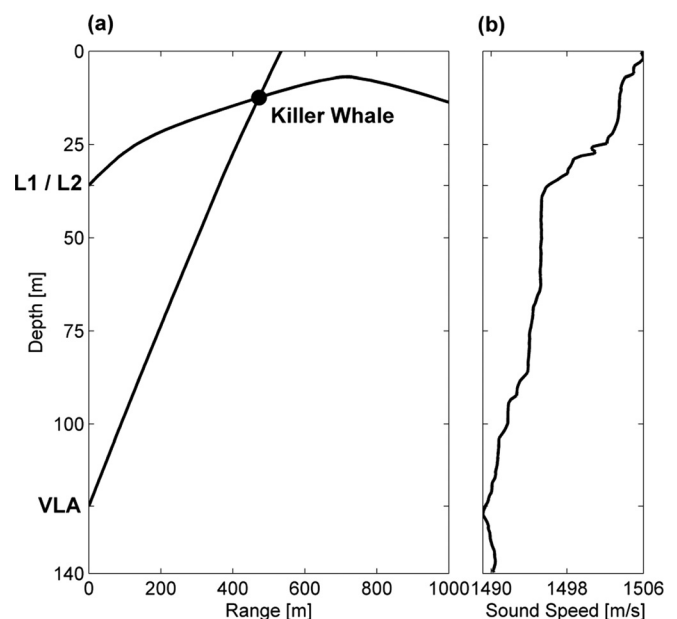


FIG. 4. Intersection of rays (a) provides a range and depth estimate for a clicking killer whale (black circle). The vertical arrival angles at the L-shaped arrays and VLAs were used as start angles for two rays, which were back-propagated using the measured sound velocity profile (b) to account for refraction.

TDOA sensitivity) for each of the legs. However, for the range and depth estimation the vertical leg of L1 was not used because it has a smaller aperture and significantly higher noise levels than the vertical leg of L2.

### 3. Bearing

Using the TDOA method and Eq. (1), angles to the clicks are estimated using the horizontal components of L1 and L2, respectively (Fig. 5). Hydrophone pairs 5–6 for L1 and 4–6 for L2 were used to obtain bearings. These angles are mapped to horizontal bearings to account for the bias resulting from animal locations that are above or below the depth of the horizontal leg of L1 and L2. With the vertical angle  $\beta_{\text{ver}}$  obtained from the vertical component for a click and the direction cosines, the angle from the horizontal component  $\beta_{\text{hor}}$  can be mapped to a horizontal bearing  $\beta'_{\text{hor}}$ ,

$$\beta'_{\text{hor}} = \tan^{-1} \left[ \frac{\cos(\beta_{\text{ver}})}{1 - [\cos(\beta_{\text{ver}}) + \cos(\beta_{\text{hor}})]} \right]. \quad (2)$$

With the known orientation of the horizontal component of L1 and L2, the horizontal bearing  $\beta'_{\text{hor}}$  can be converted into a bearing with a scale ranging from 0° (N) over 180° (S) to 360° (N) with respect to FLIP.

Due to the left-right ambiguity typical of line arrays, each horizontal component of L1 and L2 provides a set of two possible bearings (Fig. 5). Since the clicking animals are typically much farther away than several times the distance between L1 and L2, crossing the bearings will give inaccurate locations. However, one of the bearings from L2 will line up with one of the bearings from L1 providing an unambiguous bearing to the sound source (Fig. 5).

### D. Associating pulsed calls with individual killer whales

The pulsed calls of the killer whales have a lower signal-to-noise ratio (SNR) than the clicks and are longer in

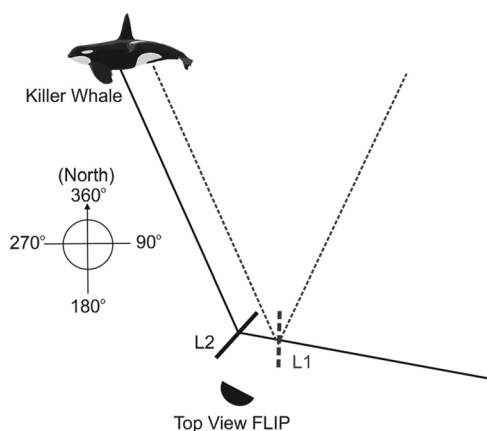


FIG. 5. Bearings of the horizontal components for the L1 and L2 arrays are represented by the dashed line and the solid line, respectively. Each array measures two possible bearings due to the left-right ambiguity common to line arrays. This ambiguity is resolved by selecting the bearings that give consistent locations between L1 and L2.

duration (several hundred milliseconds), which leads to an insufficient time resolution of the TDOA for the spacing of the three individual arrays with a maximal possible TDOA of 1 ms. This makes it difficult to localize them. However, since L2 and VLA are 86 m apart, the pulsed calls were cross-correlated between these two arrays to provide a sufficient TDOA time resolution. In addition, the localized clicks (Sec. II A) of each killer whale are also cross-correlated between L2 and the VLA, yielding one set of click TDOAs for each of the five killer whales. Then, the TDOA of a pulsed call at a given time is compared to the click TDOAs of each of the five killer whales around that time to associate the pulsed call with one of the five killer whales. If the difference between that pulsed call TDOA and the click TDOAs of a killer whale is smaller than 3 ms and the TDOA differences to all other killer whales are greater than 6 ms, a pulsed call is considered to be unambiguously associated with a particular killer whale track. For that reason, the location of the pulsed call is approximated by the location of a click produced by the associated killer whale at about the time of the pulsed call. This procedure eliminates the need to localize pulsed calls on the individual small aperture arrays and would also work for whistles since their duration is similar to the pulsed calls.

### E. Localizing high-frequency modulated calls

The HFM signals occur during times when no click tracks are available and therefore the method in the previous section is not applicable. However, the HFM calls were recorded on the four seafloor HARP and on the FLIP arrays, which form a large aperture array with spacing ranging from one to two kilometers. The TDOAs of the HFM calls between the HARP and FLIP were manually picked. The three-dimensional localization was conducted using the hyperbolic fixing algorithm (Spiesberger and Fristrup, 1990) assuming a constant sound speed profile. Since the rays travel rather straight paths due to greater vertical angles resulting from 300–400 m depth difference between the HARP and the killer whales, in contrast to 0–40 m depth difference between L1/L2 and the killer whales, refraction effects therefore were neglected for the large aperture seafloor array.

### F. Source levels

Peak to peak source levels for each localized click, pulsed and HFM call were calculated from the sum of the peak to peak received level ( $RL_{\text{pp}}$ ) and the transmission loss (TL). We assume spherical spreading, since the ranges to the killer whales ( $r$ ) are typically less than the water depth. We also include a frequency dependent attenuation coefficient ( $\alpha$ ). The TL is combined with the  $RL_{\text{pp}}$  to estimate the peak to peak source level ( $SL_{\text{pp}}$ ) in dB re 1  $\mu\text{Pa}$  @ 1 m from

$$SL_{\text{pp}} = RL_{\text{pp}} + 20\log_{10}(r[m]) + \alpha \times r[m]/1000, \quad (3)$$

where  $\alpha$  is taken to be 3  $\text{dBkm}^{-1}$  at 20 kHz for the clicks and 5  $\text{dBkm}^{-1}$  at 25 kHz for the HFM calls (Ainslie and

McColm, 1998). The frequency attenuation term is neglected for the pulsed calls due to the low attenuation at frequencies below 10 kHz.

The peak to peak received level in dB re  $1 \mu\text{Pa}$  of each killer whale sound is calculated from the maximum and minimum of its bandpass-filtered calibrated pressure time series  $p(t)$  recorded by the L2 array hydrophone #4 using the reference pressure  $p_0$  of  $1 \mu\text{Pa}$

$$\text{RL}_{\text{pp}} = 10 \log_{10} \left( \frac{\max\{p(t)\} + |\min\{p(t)\}|}{p_0} \right)^2. \quad (4)$$

Calibrations of the FLIP arrays and HARP's hydrophone sensitivities were performed at the U.S. Navy's Transducer Evaluation Center facility in San Diego, CA and at the Scripps Whale Acoustics Laboratory at the University of California, San Diego.

### III. RESULTS

Approximately one hour after sunset on 11 November 2008, a group of five killer whales were tracked using their emitted sounds and the algorithms described above. Their echolocation clicks were short duration ( $<250 \mu\text{s}$ ) signals with peak energy in the 10–30 kHz band. These clicks showed variations on short time scales that may result from beam pattern effects, with higher amplitude and higher

bandwidth clicks assumed to be more nearly received on-axis [Figs. 6(a) and 6(b)]. HFM signals were moderate duration ( $\sim 90 \text{ms}$ ) frequency modulated downswept signals around 20 kHz with visible harmonics [Fig. 6(c)]. Pulsed calls were long duration ( $\sim 0.5 \text{s}$ ) rapidly modulated tones often with both side-banding and harmonics (Fig. 7).

Detailed bearings, ranges and depths of the echolocation clicks fall along discrete tracks over a period of about 5 min. A single track is shown in Fig. 8; individual range and depth estimates are fitted with polynomials to aid with interpretation. The peak to peak source level estimates of the clicks [Fig. 8(d)] vary between 170 and 205 dB re  $1 \mu\text{Pa}$  @ 1 m, in good agreement with previous estimates (Simon *et al.*, 2007), but about 20 dB lower than what has been reported for Northeast Pacific resident killer whales (Au *et al.*, 2004).

Three-dimensional tracks for five killer whales were estimated using over 700 clicks, 9 pulsed calls and four HFM calls from about an eight minute period (Fig. 9). Individuals from the group were first localized about 350 m east to southeast of FLIP heading northwest. Killer whales A and B transit south of FLIP, while killer whales C, D, and E travel east of FLIP. As all of the killer whales get closer to FLIP, they decrease their depth from about 40 m to less than 5 m when they reach their closest point of approach (CPA) to FLIP. The minimum distance of the killer whales to FLIP was always greater than 100 m. The durations of the killer whale tracks vary between 2–5 min. Around 02:43:41 GMT,

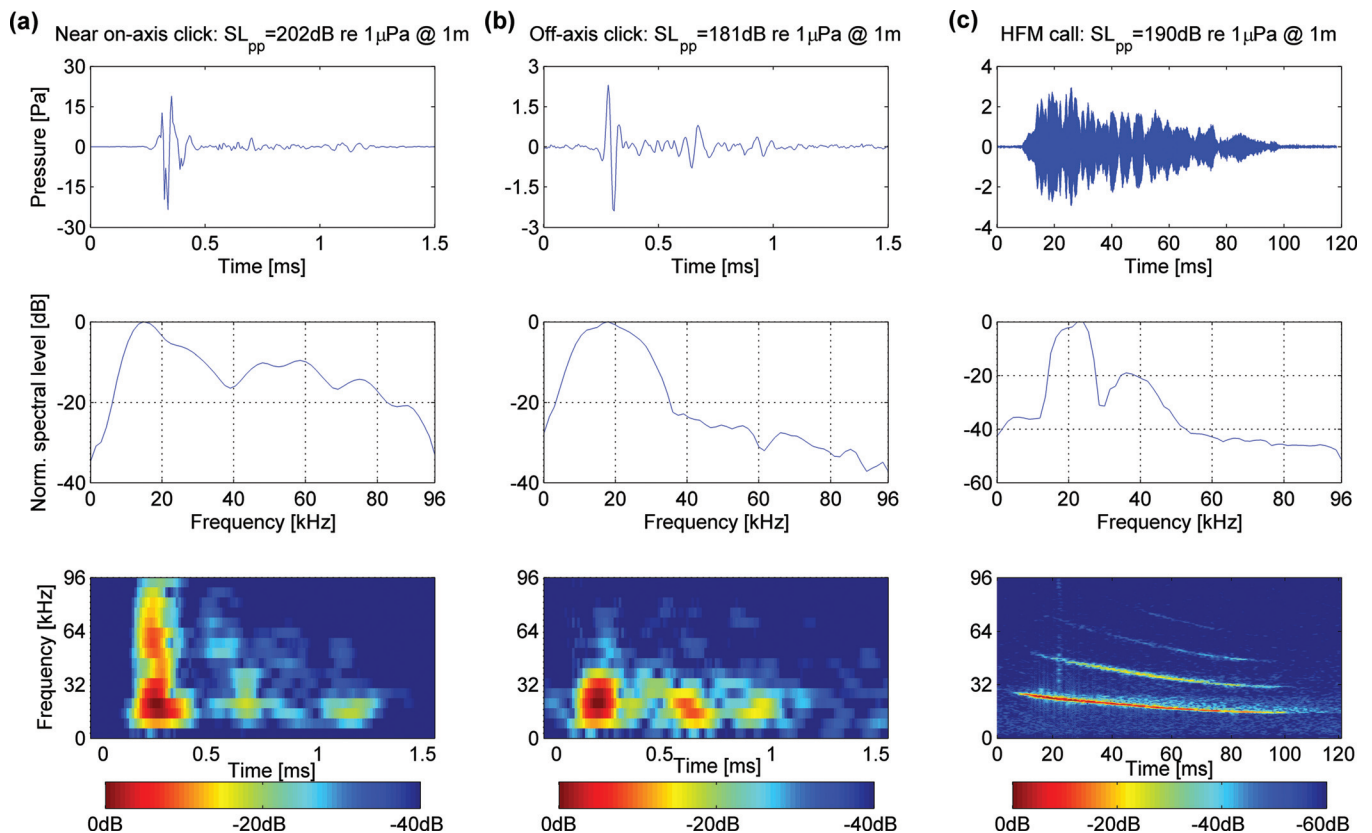


FIG. 6. Pressure time series, normalized spectral densities and spectrograms (top to bottom) of a received near on-axis click (a), an off-axis click (b), and an HFM call (c). Peak to peak source levels ( $\text{SL}_{\text{pp}}$ ) are obtained from the pressure time series using Eq. (3). Spectrograms were calculated with Hamming windows, 32 and 512 sample FFTs with 95% overlap for the clicks and HFM call, respectively. Spectrograms and spectral densities were normalized by their maxima. Both clicks in (a) and (b) are about  $250 \mu\text{s}$  long and have two multipath arrivals about 0.5 ms and 0.8 ms after the first arrival. The HFM call in (c) is a frequency modulated downsweep around 20 kHz with 3 harmonics.

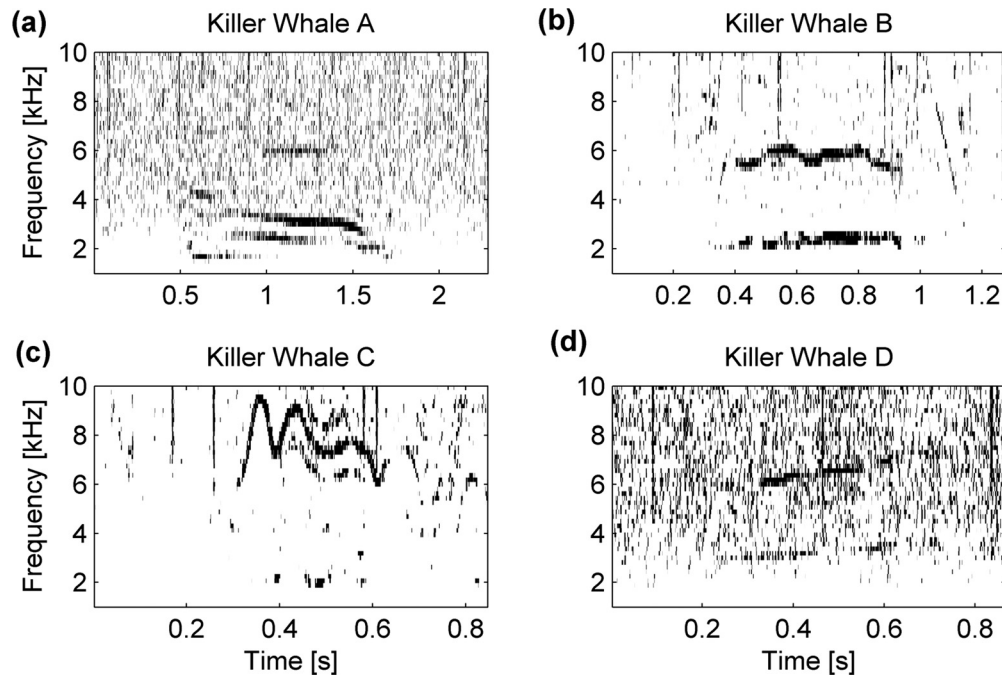


FIG. 7. Spectrograms for the last localized pulsed calls for the killer whale tracks A (a), B (b), C (c), and D (d) (see Fig. 9). Spectrograms were computed with 512 sample FFTs with 90% overlap using Hamming windows.

the tracks of killer whales A and B appear to merge into one track, leaving it unclear whether the track belongs to killer whale A or B or both. The magnitude of the velocity vector of the killer whales varies between 1 and 10  $\text{kmh}^{-1}$ . When passing FLIP, whales C and A/B slow down temporarily from 6 to 2  $\text{kmh}^{-1}$ , while whales D and E travel at average speeds of 9 and 5  $\text{kmh}^{-1}$ , respectively.

The HFM calls were localized approximately 500 m northwest of FLIP with peak to peak source level estimates ranging between 185 and 193 dB re 1  $\mu\text{Pa}$  @ 1 m [Fig. 6(c)]. These locations further suggest the overall northwest movement of the killer whale group.

The peak to peak source levels of the last pulsed call from the killer whales A, B, C, and D in Fig. 9 were 146, 153, 158, and 150 dB re 1  $\mu\text{Pa}$  @ 1 m, respectively (Fig. 7). Although there are variations in the degree of frequency modulation, number of harmonics and call length, no characteristics to distinguish individuals could be established due to the limited number of pulsed calls per track (Fig. 9).

#### IV. DISCUSSION

The accuracy of the killer whale sound localizations depends on the knowledge of the array element locations, the accuracy of the calculated TDOA based on the time-bandwidth product of each killer whale sound type and the knowledge of the sound velocity field.

Although the inter-element spacing of each of the arrays are known with an accuracy of less than one centimeter and the array orientation was calibrated by tracking ship noise from known GPS locations, L1 and L2 potentially could be vertically inclined and horizontally rotated by an unknown small angle due to their mounting configuration and ocean

currents leading to increased uncertainty in vertical angles and bearings. Equipping the arrays with a compass and a tilt sensor would help to monitor the array orientations in future deployments. In addition, the vertical components of L2 and the VLA used for the range and depth estimation were not vertically aligned and were off-axis by less than 10 m, which contributes to the uncertainty of the range and depth estimates for the clicks by less than 5 m, respectively.

The hydrophone spacing of L1, L2 and VLA provides maximum TDOAs around 1 ms allowing clicks, which are typically short duration ( $<250 \mu\text{s}$ ), to be used for angle estimates with errors smaller than  $2^\circ$ . However, all other killer whale sounds (HFM and pulsed calls) have a comparably smaller bandwidth, lower SNR and longer duration than the clicks, preventing their being used for cross-correlation, which would result in large angle uncertainties. Therefore, a frequency-domain beamformer for L1 and L2 was investigated by splitting the L-shape up into two line arrays with three elements each or by utilizing the entire L-shape with all six hydrophones as a two-dimensional array to exploit the maximum possible array gain. In either case, the results were unsatisfactory since the wavelengths of the pulsed calls are too large for the array spacing and the bandwidth of the pulsed calls is usually too small to resolve the spatial aliasing by frequency averaging of the beamformer outputs (Thode *et al.*, 2000). To overcome these limitations, the pulsed calls were cross-correlated between hydrophones of different arrays; for example, cross-correlating the signal from one hydrophone of L2 with one from VLA. Pulsed calls, which often overlap with clicks, were cross-correlated only during periods free of clicks to prevent contamination from the higher SNR of the clicks. Due to a varying SNR of the pulsed calls and occasionally similar click TDOAs for different animals around the same time instance, only a

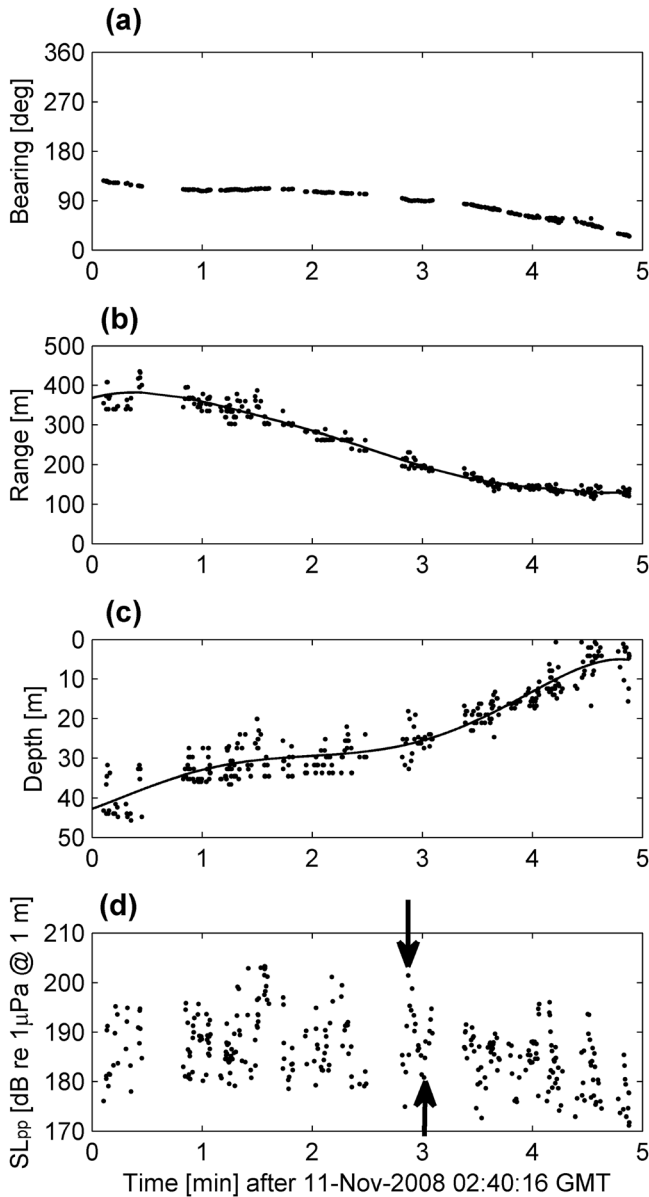


FIG. 8. Bearing (a), range (b), depth (c), and peak to peak source level (d) estimates for the click track from killer whale C. Ranges and depths were smoothed with polynomial functions represented by the solid lines in (b) and (c). The down and upward pointing arrow in (d) around the 3rd min highlights the clicks used in Fig. 6 (a) and (b) as a near on-axis and off-axis click, respectively.

fraction of the pulsed calls could be confidently and unambiguously associated with specific animals (9 out of 60 detected pulsed calls).

The location error of the HFM calls was about 150 m assuming 5 m uncertainty in the positions of FLIP and the four HARPs, 10 ms uncertainty in the TDOAs and  $20 \text{ m s}^{-1}$  uncertainty in the sound speed. However, the location errors of the HFM calls contribute less than 4 dB to their source level error because of the logarithmic relationship between  $TL$  and range at these distances with respect to FLIP ( $\sim 500 \text{ m}$ ).

For the higher-resolution three-dimensional click localization method, a range and bearing independent sound speed field was assumed [Fig. 4(b)]. The sound speed profile was obtained just 8 h before the killer whale tracks.

Depending on the sound speed profile, the array locations and the clicking killer whale locations, this method provides more accurate ranges and depths than simply intersecting straight lines starting with the TDOA measured angles of L2 and VLA. For example, for the measured sound speed profile [Fig. 4(a)] and a killer whale 264 m away at a depth of 19 m, the error of the location based on simply crossing the vertical angles is 30 and 15 m for range and depth, respectively.

The scatter in the range and depth estimates from the clicks was greater than for the bearing estimates because of source and receiver geometry. For example, plane waves arriving nearly perpendicular to array components will have TDOAs that are more sensitive to changes in angle than waves arriving along the array axis because of the cosine relation in Eq. (1). This was the case for the vertical arrays when the killer whales were far away or at the array depth. A polynomial smoothing function for the range and depth estimates was chosen over a Kalman filter because it is easy to implement and provides clean large-scale tracks at the cost of averaging out possible fine-scale movements, i.e., possible 10 m up and down dive within 10 s as shown in Fig. 8(c). Testing if a particle or even a Kalman filter could separate out these fine-scale movements from the measurement noise, is a subject for further investigation.

Only a few surface or bottom reflections were found in the recordings, preventing multipath localization techniques from being used. Furthermore, the three-dimensional click localization method requires that the same killer whale click was received on all three arrays deployed from FLIP. After the killer whales passed FLIP, tracking was discontinued because the number of clicks on all arrays was significantly reduced. The shallow depths near the CPA suggest the whales were surfacing, perhaps to breathe, and therefore may have reduced their clicking rates. In addition, clicks are highly directional and after the closest-point-of-approach with FLIP, the headings of the click beams were no longer directed toward the arrays.

The estimated click peak to peak source levels vary between 170 and 205 dB re  $1 \mu\text{Pa} @ 1 \text{ m}$  probably because of the click beam pattern and the orientation of the killer whale with respect to the array (L2). For example, the source level rose and fell by about 20 dB over short periods suggesting the click beam angle was swept through the array direction [Fig. 8(d)] rather than caused by location error, since the logarithmic relationship between transmission loss and range limits the error in source level to less than 3 dB. Therefore, the near on-axis and off-axis clicks in Figs. 6(a) and 6(b) were recruited from killer whale C as it is assumed to increasingly point its acoustic beam towards array L2 with a maximum  $SL_{pp}$  of 202 dB re  $1 \mu\text{Pa} @ 1 \text{ m}$  (considered to be near-on axis) and then away from the array with a minimum  $SL_{pp}$  of 181 dB re  $1 \mu\text{Pa} @ 1 \text{ m}$  (considered to be off-axis) between 02:43:00 GMT and 02:43:16 GMT [Fig. 8(d)]. The decrease of energy at higher frequencies ( $>40 \text{ kHz}$ ) for the off-axis click [Fig. 6(b)] compared to the near on-axis click [Fig. 6(a)] is another suggestion for directionality of these clicks. The consistent multipath arrivals for the near on-axis and off-axis clicks, which are identical across all channels of

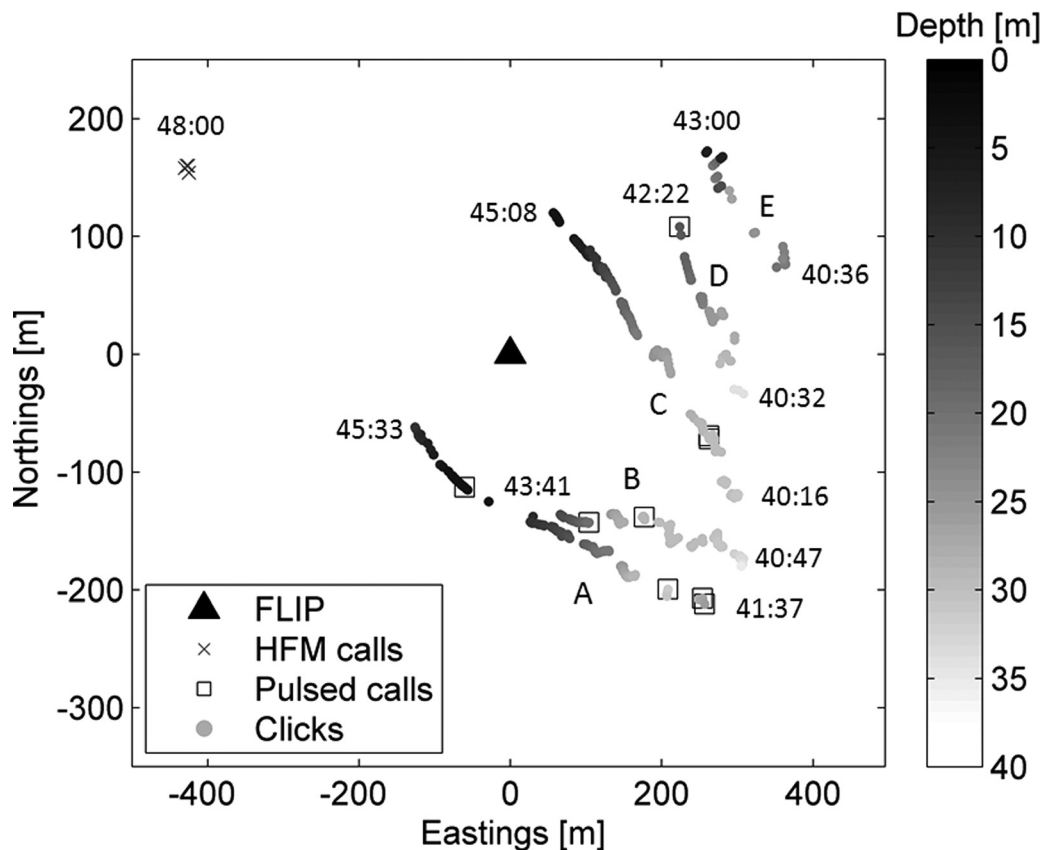


FIG. 9. Three-dimensional tracks of the killer whales A, B, C, D, and E relative to FLIP. Depths of click localizations are represented by the grayscale bar on the right. Boxes indicate pulsed calls. High-frequency modulated (HFM) call localizations are shown as cross marks. Times are in minute-second format (mm:ss) after 2008-11-11 02:00:00 GMT.

array L2, suggest that they are not caused by the arrays but instead might be created by the sound production mechanism of the killer whale itself, as described for other clicking toothed whales (Cranford *et al.*, 2011).

## V. CONCLUSIONS

A three-dimensional propagation-model based passive acoustic tracking method for broadband echolocation clicks was developed for two L-shaped arrays and one VLA deployed from FLIP. Using these small aperture arrays together with the medium-aperture array from L2 to VLA and the large aperture between the FLIP arrays and the four HARPes around FLIP, a group of five offshore killer whales was tracked by using their emitted clicks as well as their pulsed and HFM calls. Based on the tracks, the speed of each killer whale and the source levels for all three call types were estimated.

These acoustic methods provide a tool to track and study other delphinid species. If conducted during daylight hours, the acoustic tracks and behaviors also can be compared with the visually observed surface behaviors to provide a more comprehensive understanding of their habitat use than by either technique individually.

## ACKNOWLEDGMENTS

Funding for this research was provided by the U.S. Navy CNO-N45 and the Naval Postgraduate School; we

thank Frank Stone, Ernie Young, Curt Collins, and John Joseph for support and assistance. We thank the Scripps Whale Acoustics Lab members, especially Ethan Roth, Chris Garsha, and Brent Hurley for help with data collection as well as Bill Hodgkiss and Greg Campbell for useful discussions. Furthermore, we thank the FLIP crew members, particularly Bill Gaines, Captain Tom Golfinos, Paul Porcioncula, and Greg Viehmann. We also thank Amalis Riera, Volker Deecke, and John Ford for their efforts in determining the killer whale ecotype.

- Ainslie, M., and McColm, J. (1998). "A simplified formula for viscous and chemical absorption in sea water." *J. Acoust. Soc. Am.* **103**, 1671–1672.
- Au, W. W. L., Ford, J. K. B., Horne, J. K., and Allman, K. A. N. (2004). "Echolocation signals of free-ranging killer whales (*Orcinus orca*) and modeling of foraging for chinook salmon (*Oncorhynchus tshawytscha*)," *J. Acoust. Soc. Am.* **115**, 901–909.
- Barlow, J., and Taylor, B. L. (2005). "Estimates of sperm whale abundance in the northeastern temperate Pacific from a combined acoustic and visual survey," *Marine Mammal Sci.* **21**, 429–445.
- Barrett-Lennard, L. G., Ford, J. K. B., and Heise, K. A. (1996). "The mixed blessing of echolocation: Differences in sonar use by fish-eating and mammal-eating killer whales," *Anim. Behav.* **51**, 553–565.
- Chen, C.-T., and Millero, F. J. (1977). "Speed of sound in seawater at high pressures," *J. Acoust. Soc. Am.* **62**, 1129–1135.
- Cranford, T. W., Elsberry, W. R., Van Bonn, W. G., Jeffress, J. A., Chaplin, M. S., Blackwood, D. J., Carder, D. A., Kamolnick, T., Todd, M. A., and Ridgway, S. H. (2011). "Observation and analysis of sonar signal generation in the bottlenose dolphin (*Tursiops truncatus*): Evidence for two sonar sources," *J. Exp. Mar. Biol. Ecol.* **407**, 81–96.
- Fisher, F. H., and Spiess, F. N. (1963). "Flip-Floating Instrument Platform," *J. Acoust. Soc. Am.* **35**, 1633–1644.

- Ford, J. K. B. (1989). "Acoustic behaviour of resident killer whales (*Orcinus orca*) off Vancouver Island, British Columbia." *Can. J. Zool.* **67**, 727–745.
- Fristrup, K. M., and Watkins, W. A. (2004). *Characterizing Acoustic Features of Marine Mammal Sounds* (Woods Hole Oceanographic Institute, Woods Hole, MA), Vol. 1992.
- Kaiser, J. F. (1990). "On a simple algorithm to calculate the 'energy' of a signal," *International Conference on Acoustics, Speech, and Signal Processing*, IEEE, Albuquerque, NM, Vol. 1, pp. 381–384.
- Kandia, V., and Stylianou, Y. (2006). "Detection of sperm whale clicks based on the Teager–Kaiser energy operator," *Appl. Acoust.* **67**, 1144–1163.
- Lagarias, J., Reeds, J., Wright, M., and Wright, P. (1998). "Convergence properties of the Nelder–Mead simplex method in low dimensions," *SIAM J. Optimiz.* **9**, 112–147.
- Lewis, T., Gillespie, D., Lacey, C., Matthews, J., Danbolt, M., Leaper, R., McLanaghan, R., and Moscrop, A. (2007). "Sperm whale abundance estimates from acoustic surveys of the Ionian Sea and Straits of Sicily in 2003," *J. Mar. Biol. Assoc. U.K.* **87**, 353–357.
- Nosal, E. M., and Frazer, L. N. (2007). "Sperm whale three-dimensional track, swim orientation, beam pattern, and click levels observed on bottom-mounted hydrophones," *J. Acoust. Soc. Am.* **122**, 1969–1978.
- Porter, M. B., and Buckner, H. P. (1987). "Gaussian beam tracing for computing ocean acoustic fields," *J. Acoust. Soc. Am.* **82**, 1349–1359.
- Roch, M. A., Klinck, H., Baumann-Pickering, S., Mellinger, D. K., Qui, S., Soldevilla, M. S., and Hildebrand, J. A. (2011). "Classification of echolocation clicks from odontocetes in the Southern California Bight," *J. Acoust. Soc. Am.* **129**, 467–475.
- Samarra, F. I. P., Volker, B. D., Katja, V., Marianne, H. R., Rene, J. S., and Patrick, J. O. M. (2010). "Killer whales (*Orcinus orca*) produce ultrasonic whistles," *J. Acoust. Soc. Am.* **128**, EL205–EL210.
- Simon, M., Wahlberg, M., and Miller, L. A. (2007). "Echolocation clicks from killer whales (*Orcinus orca*) feeding on herring (*Clupea harengus*)," *J. Acoust. Soc. Am.* **121**, 749–752.
- Simonis, A. E., Baumann-Pickering, S., Oleson, E., Melcon, M. L., Gassmann, M., Wiggins, S. M., and Hildebrand, J. A. (2012). "High-frequency modulated signals of killer whales (*Orcinus orca*) in the North Pacific," *J. Acoust. Soc. Am.* **131**, EL295–EL301.
- Spiesberger, J. L., and Fristrup, K. M. (1990). "Passive Localization of Calling Animals and Sensing of their Acoustic Environment Using Acoustic Tomography," *Am. Nat.* **135**, 107–153.
- Thode, A. (2005). "Three-dimensional passive acoustic tracking of sperm whales (*Physeter macrocephalus*) in ray-refracting environments," *J. Acoust. Soc. Am.* **118**, 3575.
- Thode, A., Norris, T., and Barlow, J. (2000). "Frequency beamforming of dolphin whistles using a sparse three-element towed array," *J. Acoust. Soc. Am.* **107**, 3581–3584.
- Thode, A., Skinner, J., Scott, P., Roswell, J., Straley, J., and Folkert, K. (2010). "Tracking sperm whales with a towed acoustic vector sensor," *J. Acoust. Soc. Am.* **128**, 2681.
- Tiemann, C. O., Thode, A. M., Straley, J., O'Connell, V., and Folkert, K. (2006). "Three-dimensional localization of sperm whales using a single hydrophone," *J. Acoust. Soc. Am.* **120**, 2355.
- Wiggins, S. M., and Hildebrand, J. A. (2007). "High-frequency Acoustic Recording Package (HARP) for broad-band, long-term marine mammal monitoring," in *International Symposium on Underwater Technology 2007 and International Workshop on Scientific Use of Submarine Cables & Related Technologies 2007*, IEEE, Tokyo, Japan, pp. 551–557.
- Wiggins, S. M., McDonald, M. A., and Hildebrand, J. A. (2012). "Beaked whale and dolphin tracking using a multichannel autonomous acoustic recorder," *J. Acoust. Soc. Am.* **131**, 156–163.